Icarus 319 (2019) 33–42

Contents lists available at ScienceDirect

Icarus

journal homepage: www.elsevier.com/locate/icarus

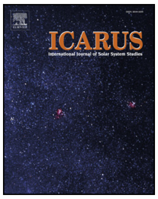

Surface deposition of the Enceladus plume and the zenith angle of emissions

Ben S. Southworth*[a,c], Sascha Kempf[b,c], Joe Spitale[d]

[a] Department of Applied Mathematics, University of Colorado Boulder, United States
[b] Physics Department, University of Colorado Boulder, United States
[c] Laboratory for Atmospheric and Space Physics, University of Colorado Boulder, United States
[d] Planetary Science Institute, United States

ARTICLE INFO

Keywords:
Enceladus
Plume
Surface deposition

ABSTRACT

Since the discovery of an ice particle plume erupting from the south polar terrain on Saturn's moon Enceladus, the geophysical mechanisms driving its activity have been the focus of substantial scientific research. The pattern and deposition rate of plume material on Enceladus' surface is of interest because it provides valuable information about the dynamics of the ice particle ejection as well as the surface erosion. Surface deposition maps derived from numerical plume simulations by Kempf et al. (2010) have been used by various researchers to interpret data obtained by various Cassini instruments. Here, an updated and detailed set of deposition maps is provided based on a deep-source plume model (Schmidt et al., 2008), for the eight ice-particle jets identified in Spitale and Porco (2007), the updated set of jets proposed in Porco et al. (2014), and a contrasting curtain-style plume proposed in Spitale et al. (2015). Methods for computing the surface deposition are detailed, and the structure of surface deposition patterns is shown to be consistent across changes in the production rate and size distribution of the plume. Maps are also provided of the surface deposition structure originating in each of the four Tiger Stripes. Finally, the differing approaches used in Porco et al. (2014) and Spitale et al. (2015) have given rise to a jets vs. curtains controversy regarding the emission structure of the Enceladus plume. Here we simulate each, leading to new insight that, over time, most emissions must be directed relatively orthogonal to the surface because jets "tilted" significantly away from orthogonal lead to surface deposition patterns inconsistent with surface images.

Data for maps are available in HDF5 format for a variety of particle sizes at http://impact.colorado.edu/southworth_data.

1. Introduction

In 2005 the Cassini mission made the exciting discovery of a water-vapor and ice-particle plume erupting from the south polar terrain on Saturn's icy moon Enceladus (Dougherty et al., 2006; Hansen et al., 2006; Porco et al., 2006; Spahn et al., 2006; Spencer et al., 2006). Multiple Cassini traversals through the plume allowed Cassini in-situ instruments to collect samples of the emerging vapor (Waite et al., 2009) and ice particles (Postberg et al., 2009), the larger of which likely originate from the boiling surface of the moon's subsurface ocean (Postberg et al., 2011). Since then much research has been devoted to understanding the Enceladus plume and its driving mechanism, for example, see Brilliantov et al. (2008); Gao et al. (2016); Hurford et al. (2007); Schmidt et al. (2008). There is convincing evidence that the plume is by far the strongest source of E-ring particles (for example, Spahn et al., 2006; Horányi et al., 2009) and also the dominant source of the resurfacing of Enceladus (for example, Jaumann et al., 2009; Kempf et al., 2010). However, there remain open questions about the plume, some of which may be addressed by examining surface deposits.

The purpose of this work is two-fold. First, we provide simulated surface deposition data resulting from the three primary proposals for plume emission structure: the eight jets identified in Spitale and Porco (2007), an updated set of approximately 100 sources identified in Porco et al. (2014), and a contrasting "curtain-like" plume proposed in Spitale et al. (2015). Multiple particle sizes from 0.6 – 15 μm are simulated for each source location, and data are generated on the impact flux in particles/sec/m^2 and mass deposition in mm/year across the surface of Enceladus. Initial simulated maps of surface deposition from the Enceladus plume published in Kempf et al. (2010) have received interest from the larger research community (for example, Di Sisto and Zanardi, 2016; Nahm and Kattenhorn, 2015; Scipioni et al., 2017) and,

---

* Corresponding author at: Department of Applied Mathematics, University of Colorado at Boulder, United States.
E-mail address: ben.s.southworth@gmail.com (B.S. Southworth).

https://doi.org/10.1016/j.icarus.2018.08.024
Received 29 January 2018; Received in revised form 22 August 2018; Accepted 28 August 2018
Available online 05 September 2018
0019-1035/ © 2018 Elsevier Inc. All rights reserved.

here, we provide a more complete set of maps and data with respect to source location and particle size. Using the newly generated surface data for a curtain-style plume (Spitale et al., 2015) and the ~ 100 discrete jets proposed in Porco et al. (2014), we provide new insight into the zenith angle of plume emissions, that is, the “tilt” of the jets. Specifically, comparing simulated surface deposition patterns with the surface pattern seen in IR/UV images (Schenk et al., 2011) indicates that highly tilted jets (zenith angle $\gg 15^\circ$) identified in Porco et al. (2014) are not contributing substantially to surface deposition; that is, the unique signature of highly tilted jets is not apparent in surface images. Potential reasons for this are discussed in Section 4. The most likely explanation is that highly tilted jets experience short lifetimes and are not active long enough to develop observable surface features.

A background on the plume model and simulations is given in Section 2, along with a description of the data. Details on computing impact flux and surface deposition can be found in the Appendix. Maps of surface deposition as a function of time are given in Section 3. Data for surface maps are available in HDF5 format (The HDF Group, 2000–2010) at http://impact.colorado.edu/southworth_data , and are summarized in the following table:

Section 4 introduces the jets vs. curtains controversy and provides evidence that, regardless of whether emissions originate from discrete jets or in a continuous curtain-style emission, the zenith angle of emissions is largely close to orthogonal to the surface. Implications and other open questions that surface deposition may provide insight towards are discussed in Section 5.

2. Plume model

Here we assume that the Enceladus plume is fed by a “deep-source” mechanism (Brilliantov et al., 2008; Schmidt et al., 2008; Postberg et al., 2011), where fractures in Enceladus' icy crust extend down to a liquid-water reservoir. Particles then condense and are accelerated though a back-pressurized gas flow exiting the fracture, for which the particle velocity upon ejection takes the following distribution[1]

$$p(v|r) = \left(1 + \frac{r}{r_c}\right)\frac{r}{r_c}\frac{v}{v_{gas}^2}\left(1 - \frac{v}{v_{gas}}\right)^{\frac{r}{r_c}-1}, \tag{1}$$

where

$$\int_0^{v_{gas}} p(v|r)dv = 1, \tag{2}$$

The velocity distribution (Eq. (1)) assumes that particle velocities cannot be larger than the gas velocity, v_{gas}, hence the normalization integral in Eq. (2) over $[0, v_{gas}]$.[2] Evidence of a deep-source plume mechanism can be found in Schmidt et al. (2008); Postberg et al. (2011) and Yeoh et al. (2015). In Eq. (1), v_{gas} is the gas velocity, and r_c the so-called critical radius, which is effectively a measure of the length of time a particle has to be reaccelerated by the gas between its final collision with a fracture wall and ejection. Particles $r < r_c$ are efficiently accelerated to velocities approaching v_{gas}, while particles $r > r_c$ move in the gas flow at average velocities less than v_{gas}. A detailed look at the critical radius, r_c, and gas velocity, v_{gas}, can be found in Schmidt et al. (2008) and Southworth et al. (2015).

In the detailed model of plume-particle speed distribution, derived in Schmidt et al. (2008), r_c and v_{gas} are actually nonlinearly coupled variables. To that end, simulations of the venting process were run in Schmidt et al. (2008) to produce a discrete probability distribution over a set of particle radii, rather than an analytical distribution with fixed r_c and v_{gas}, as in Eq. (1). For simulations of full jet- and curtain-models performed here, the discrete speed distribution developed in Schmidt et al. (2008) is used to weight particle velocities. The parameter space of v_{gas} and r_c is also explored in Section 3 by applying an analytic distribution of the form in Eq. (1), with fixed values of r_c and v_{gas}, to simulations of the eight sources in Spitale and Porco (2007). Note that for parameter values $r_c \approx 0.2\mu\text{m}$ and $v_{gas} \approx 700$ m/s, the analytic speed distribution in Eq. (1) is close to the discrete speed distribution resulting from simulations of the venting process (Schmidt et al., 2008).

The size-dependent speed distribution is consistent with a chemically stratified plume, as evidenced by data from the Cassini Cosmic Dust Analyzer (CDA) (Postberg et al., 2011), as well as surface deposition patterns that depend on particle size (Kempf et al., 2010; Scipioni et al., 2017). Particle ejection angles are assumed to be azimuthally uniform and follow a $\cos^2(\theta)$-zenith angle distribution over θ between 0° and 15°. A maximum half-angle of 15° is consistent with opening angles seen in Spitale et al. (2015), and the $\cos^2$-distribution indicative of the smooth onset, peak and decline of particle impact rates as seen by CDA (Kempf et al., 2010). A plume source is simulated by launching millions of particles from a given location and integrating their trajectories in a Saturn-centered quasi-inertial frame until each particle has either collided with Enceladus, or escaped from Enceladus and established orbit about Saturn. The equations of motion account for Saturn's gravity, Enceladus' gravity, and electromagnetic forces, including particle charging (Horányi, 1996), in a Z3-Voyager magnetic field about Saturn (Connerney, 1993). We have also implemented a magnetic field based on a local interaction model between plasma and the Enceladus plume, as proposed in Simon et al. (2011), which considers the effects of the Enceladus plume on the corotating plasma in Saturn's magnetosphere. Although the local model in Simon et al. (2011) reproduces data from the Cassini magnetometer (MAG) instrument more faithfully than a global magnetic field about Saturn, overall plume dynamics for the particle sizes considered here (> 0.6 μm) are nearly identical using a Z3-charging model, a local charging model, and no particle charging. In particular, surface deposition patterns are not affected by a change in the charging equations considered. Further details on the software used to run simulations as well as the equations of motion and underlying distributions can be found in Schmidt et al. (2008); Kempf et al. (2010); Southworth et al. (2015). In particular, the Appendix of Southworth et al. (2018) provides a detailed description of all aspects of the software and modeling techniques.

Particle sizes between $0.6 - 15$ μm are simulated for each source location, leading to $10^6 - 10^7$ particle simulations per source. Twelve sizes are simulated for the eight jets identified in Spitale and Porco (2007), and seven sizes simulated for the curtain model (Spitale et al., 2015) and updated 100 jets proposed in Porco et al. (2014). Particle trajectories are integrated until either the particle completes two orbits about Saturn without entering Enceladus' Hill sphere, or collides with the surface of Enceladus. When a particle collides with Enceladus, its position and velocity at the time of collision are saved with respect to an Enceladus-centered inertial frame (these data are available on request). All collisions for a given particle size and source location are then grouped into 1°-latitude × 1°-longitude bins, covering the surface of Enceladus. At the meridian, one bin covers an approximate square with dimensions 4.35 km × 4.35 km and a surface area of approximately 19 km^2; at the poles, one bin covers a surface area of approximately 0.17 km^2. Bins are then normalized to give the contribution of a single ejected plume particle to impact rate per m^2 in each bin. Data for each simulated particle size and jet location are stored in 360 × 180 arrays, corresponding to planetographic coordinates in western longitude. Scaling the impact flux for each bin by the size of the bin, and summing over the entire array gives the fraction of simulated particles that collided with the

---

[1] Eq. (1) includes a correction of $1/v_{gas}$ that was omitted in Schmidt et al. (2008). That correction also appeared without comment in Southworth et al. (2015).

[2] Note that, for this model, the particle velocity upon emission is effectively determined by the depth of its final collision with a fracture wall before emission. Because the expected mean free particle path is on the order of decimeters (Schmidt et al., 2008), fractures need not be “deep” for these equations to hold, as long as the driving physics remains consistent.

Download English Version:

https://daneshyari.com/en/article/10156426

Download Persian Version:

https://daneshyari.com/article/10156426

Daneshyari.com